IOP Conf. Series: Materials Science and Engineering **372** (2018) 012011 doi:10.1088/1757-899X/372/1/012011

Relationship between notch strengthening threshold and mechanical property for ductile cast iron

T Ikeda[1,3], N-A Noda[2], Y Sano[2], T Umetani[1] and N Kai[1]

[1]Research & Development Center, Hinode, Ltd., Azaiwasaki, Miyaki-cho, Miyaki-gun, Saga, 849-0101, Japan
[2]Mechanical Engineering Department, Kyushu Institute of Technology, 1-1 Sensui-cho, Tobata-ku, Kitakyushu-shi, Fukuoka 804-8550, Japan

E-mail: t_ikeda@hinodesuido.co.jp

Abstract. In this study, dynamic tensile tests were conducted at the various strain rates and temperatures for traditional ductile cast iron. Then, the notch strength σ_B^{notch} and the static tensile strength at room temperature $\sigma_{B,\ RT}^{smooth}$ were discussed in terms of the strain rate-temperature parameter R, which is known to be useful for evaluating the combined influence of strain rate and temperature. This study focuses on the notch strengthening threshold $R \geqq R_{th}$ where σ_B^{notch} is larger than $\sigma_{B,\ RT}^{smooth}$ and therefore notched components can be used safely. In other words, if $R \geqq R_{th}$, $\sigma_{B,\ RT}^{smooth}$ can be used to evaluate notched components in mechanical design to prevent the instantaneous fracture. In this study, it was found that the R_{th} value can be predicted from the static tensile property and Brinell hardness. Since the traditional ductile cast iron considered in this paper has a broad range of mechanical properties, the present approach and discussion can be applied to evaluate other materials under various temperature and strain rate.

1. Introduction

Mechanical properties of traditional ductile cast iron can be changed widely to meet the demanding requirements [1]. The higher grade of strength can be attained with increasing the pearlitic matrix. For example, the pearlite content 45 ~ 55% has the tensile strength = 500 MPa but the pearlite content 80 ~ 90% in ductile cast iron reaches tensile strength ranging over 700 MPa. The size and weight can be reduced in structures by using the high strength grade material. Meanwhile, Charpy impact absorbed energy decreases. As an example, figure 1 shows that Charpy absorbed energy decreases drastically by changing the material from JIS-FCD500 to JIS-FCD700 [2,3]. This is the main reason why industrial application is still limited for the high strength grade ductile cast iron at the room temperature or lower temperature.

However, Charpy absorbed energy cannot be directly used for the mechanical design to prevent the instantaneous fracture. The tensile strength is used as the most basic value. Therefore, a dynamic tensile test is studied for several materials [4-9]. If the strength of notched specimen is larger than the tensile strength of smooth specimen, the tensile strength of smooth specimen can be safely used to the mechanical design of the real product having notched components under the instantaneous fracture. In this paper, those strengths will be compared in terms of the strain rate-temperature parameter R [7-14]. By using this R parameter, a notch strengthening threshold value of $R \geqq R_{th}$ will be focused when the

strength of notched specimen becomes larger than the tensile strength of smooth specimen. Then, it will be shown that the R_{th} value can be predicted by the tensile strength and Brinell hardness for all types of traditional ductile cast iron.

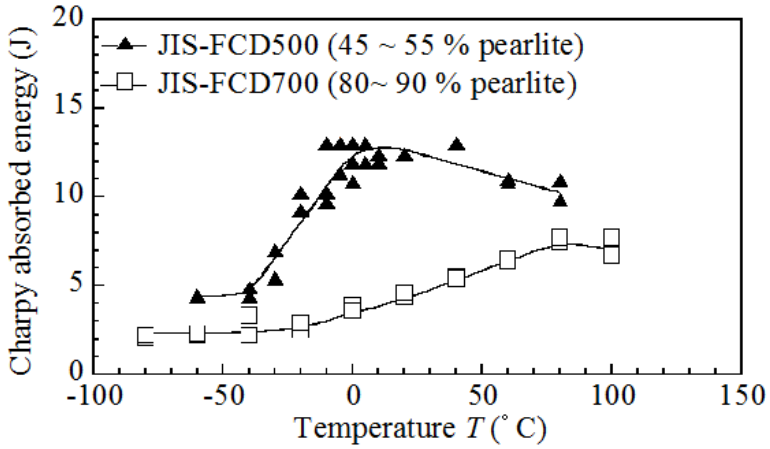

Figure 1. Charpy absorbed energy for traditional ductile cast iron [2].

2. Conditions where notch strength can be larger than smooth tensile strength

Figure 2 shows the smooth specimens and the notched round bar specimens used in the present high speed tensile test [11]. The tensile strength of smooth specimen σ_B^{smooth} and strength of notched specimen σ_B^{notch} are defined in equation (1) [9].

$$\left.\begin{aligned}\sigma_B^{smooth} &= 4\,P_{max} / \pi\, d^2 \\ \sigma_B^{notch} &= 4\,P_{max} / \pi\, d^2\end{aligned}\right\} \quad (1)$$

Here, P_{max} is maximum load (N), d is diameter of specimen. Strain rate-temperature parameter R is defined in equation (2) [7-14].

$$R = T\ \ln(A / \dot{\varepsilon}) \quad (2)$$

Here, T is temperature (K), A is 10^8 s^{-1} [10], $\dot{\varepsilon}$ is strain rate (s^{-1}). The strain rate for the smooth specimen is defined $\dot{\varepsilon}^{smooth}$. The strain rate for the notched specimen is defined $\dot{\varepsilon}^{notch}$. Those strain rates are obtained from the tensile speed v as shown in equation (3) [7-9].

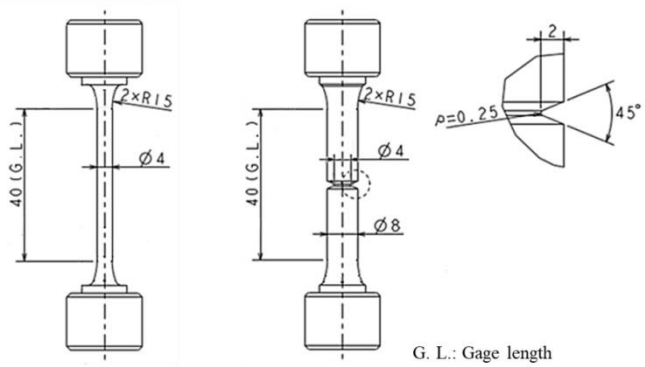

(a) (b)

Figure 2. Configuration of high speed tensile test specimen (in mm), (a) smooth specimen, and (b) notched round bar specimen.

$$\left.\begin{aligned}\dot{\varepsilon}^{\text{smooth}} &= v/\ell \\ \dot{\varepsilon}^{\text{notch}} &= K_{t\dot{\varepsilon}}\, v/\ell\end{aligned}\right\} \tag{3}$$

Here, ℓ is gauge length (40 mm). Strain rate concentration factor $K_{t\dot{\varepsilon}}$ [4-9] should be used to obtain $\dot{\varepsilon}^{\text{notch}}$ because it is difficult to measure the strain rate at the notch root. For the specimen of figure 2(b), the value of $K_{t\dot{\varepsilon}} = 9.49$ was accurately obtained in the previous study [7-9].

In the previous research, R parameter is introduced to evaluate σ_B^{notch} as a master curve [7-9]. Figure 3 shows an example of master curve of σ_B^{notch} as a function of R parameter for high silicon ferritic ductile cast iron [9]. This new material is now expected to be used as structural components [15-18]. Figure 3 also shows the static tensile strength $\sigma_{B,\ RT}^{\text{smooth}}$ for smooth specimen at room temperature. The intersection between σ_B^{notch} curve and $\sigma_{B,\ RT}^{\text{smooth}}$ line can be regarded as notch strengthening threshold R_{th}. If $R \geqq R_{th}$, σ_B^{notch} is always larger than $\sigma_{B,\ RT}^{\text{smooth}}$. Therefore, if the real products are used under $R \geqq R_{th}$, $\sigma_{B,\ RT}^{\text{smooth}}$ can be used for the mechanical design of the real product having notched components under the instantaneous fracture. This paper deals with the traditional ductile cast iron whose mechanical properties can be changed widely to meet demanding requirements by focusing on R_{th}.

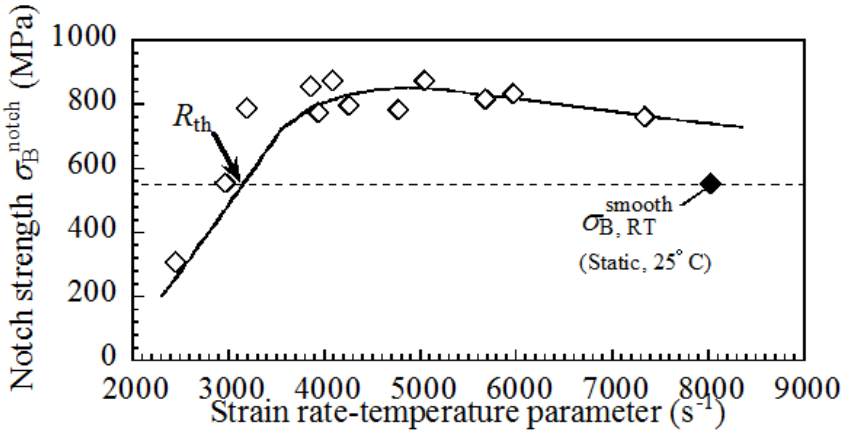

Figure 3. Influence of strain rate- temperature parameter R on σ_B^{notch} for high silicon ferritic ductile cast iron [9].

3. Experimental procedure

3.1. Preparation of specimens

In this study, we consider traditional ferrite-pearlite ductile cast irons (DCI). The tensile test was conducted according to the JIS-Z2241 standard. In addition, Brinell hardness test was conducted according to the JIS-Z2243. The tensile strength of DCI500 is approximately 500 MPa and DCI700 is approximately 700 MPa. In addition, fully pearlitic ductile cast iron (PDI) is also considered. The tensile strength of PDI is approximately 900 MPa. The pearlite ratio of DCI500 is 52.2% and DCI700 has pearlite ratio of 83.6%. PDI has fully pearlitic matrix. PDI is obtained by heat treatment indicated figure 4. The test specimen for the dynamic tensile test is taken from JIS Type Ⅱ Y-shaped blocks (JIS-G 5502).

3.2. High speed tensile test

Figure 2 shows the configuration of dynamic tensile test specimens [9]. The tests are conducted at strain rate of $2.1 \times 10^{-4} \sim 1.8 \times 10^{1}$ s^{-1}, and at temperature of -180 ~ 22°C. The experimental data of σ_B^{notch} is plotted by using the R parameter (equation (2)).

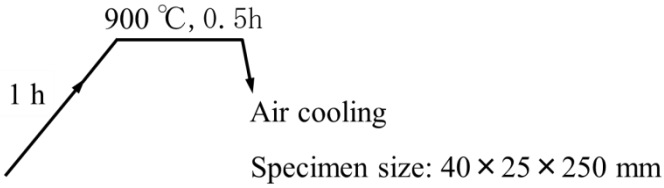

Figure 4. Normalizing condition for PDI.

4. Results and discussion

4.1. Relationship between tensile properties and pearlite area fraction

Figure 5 shows influence of pearlite area fraction on the static tensile property for smooth tensile test specimen (JIS No. 4). The static tensile strength σ_B and the 0.2% proof stress increase by increasing the pearlite area fraction. The Brinell hardness also increases by increasing the pearlite area fraction. The elongation decreases by increasing the pearlite area fraction. These results are in agreement with the other researcher's studies [2,14].

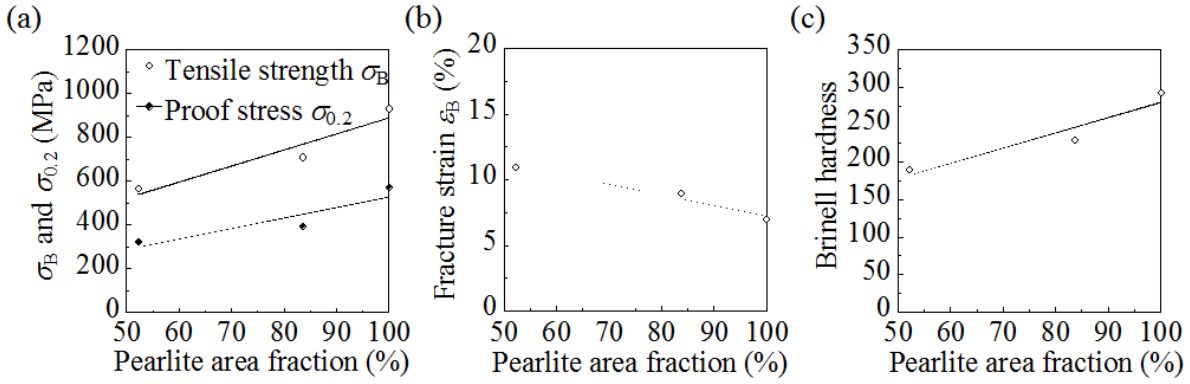

Figure 5. Influence of pearlite area fraction on static tensile properties, (a) σ_B and $\sigma_{0.2}$, (b) ε_B, (c) Brinell hardness.

4.2. Relationship between notch strengthening threshold R_{th} and static tensile property

In the dynamic tensile tests, DCI500, DCI700 and PDI showed the same tendency of the previous research on high silicon ferritic ductile cast iron in figure 3 [9]. The intersection between σ_B^{notch} curve and $\sigma_{B,\ RT}^{smooth}$ line can be regarded as notch strengthening threshold R_{th}. Figure 6 shows the relationships between the R_{th} value and the static tensile properties for the ferrite-pearlite ductile cast iron. There is a good correlation between the R_{th} value and the static tensile properties. The R_{th} value linearly increases with increasing the tensile strength and the Brinell hardness, and the R_{th} value linearly decreases with increasing the elongation. Therefore, it is considered that the R_{th} value is related to the deformation resistance of the materials.

From figure 6, the R_{th} value can be predicted from the static tensile property and Brinell hardness in the traditional ductile cast iron. Figure 7 shows the relationship between the R_{th} value and pearlite area fraction for the traditional ductile cast irons. A good correlation can be seen between the R_{th} value and pearlite area fraction. As stated earlier, in figure 5, pearlite area fraction was also correlated to the static tensile property. Therefore, a good correlation was recognized for traditional ductile cast iron in figure 6. In the traditional ductile cast iron, the increasing of the pearlite area fraction means the increasing of the deformation resistance because the pearlitic matrix doesn't have deformability. The higher grade of strength can be attained with increasing the pearlitic matrix. Therefore, it is considered

that the dependence of the mechanical property on the R_{th} value differs depending on the strengthening method in the materials.

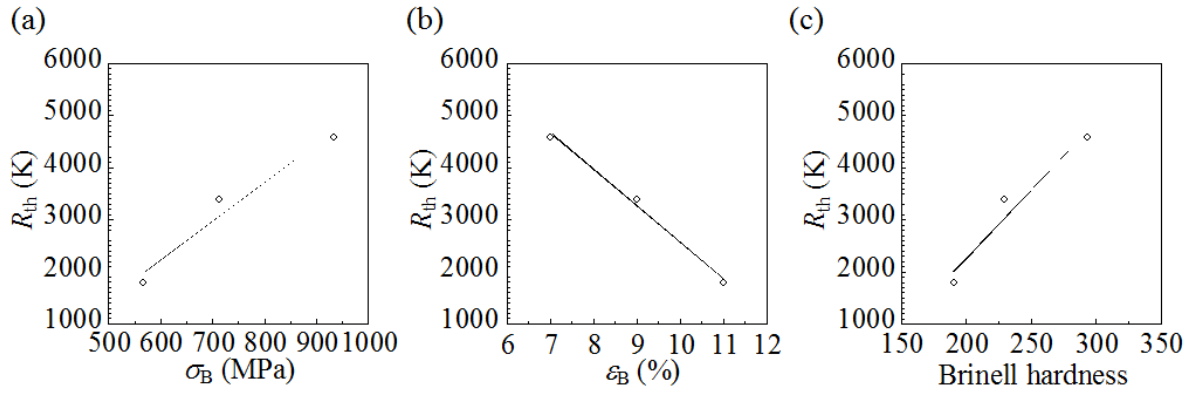

Figure 6. Relationship between R_{th} and static tensile properties, (a) σ_B, (b) ε_B, (c) Brinell hardness.

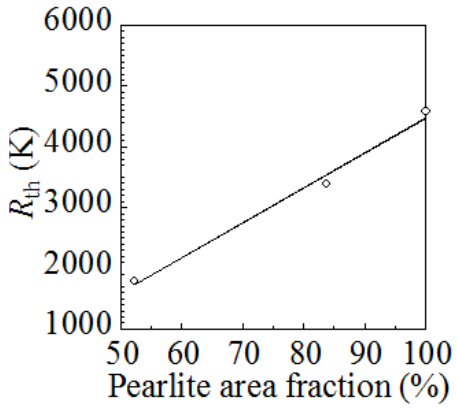

Figure 7. Relationship between R_{th} and pearlite area fraction.

5. Conclusions

In this study, for the traditional ductile cast iron, the strength of the notched specimen σ_B^{notch} was evaluated for the various strain rates and temperatures in comparison with the static tensile strength of the smooth specimen at room temperature $\sigma_{B,\ RT}^{smooth}$. The results can be applied to the mechanical design of the real product having notched components under the instantaneous fracture. From the results of this study, the conclusions can be summarized as follows.

- The intersection between σ_B^{notch} curve and $\sigma_{B,\ RT}^{smooth}$ line can be regarded as notch strengthening threshold R_{th}. If $R \geqq R_{th}$, σ_B^{notch} can be always larger than $\sigma_{B,\ RT}^{smooth}$. Therefore, if the real product having notched components is used under $R \geqq R_{th}$, $\sigma_{B,\ RT}^{smooth}$ can be used in the mechanical design to prevent the instantaneous fracture.
- The notch strengthening threshold R_{th} can be predicted from static tensile property and Brinell hardness in the traditional ductile cast iron (see figure 6).
- Since mechanical properties can be widely changed in the traditional ductile cast iron, the present discussion can be applied to evaluate other materials under various temperature and strain rate.

References

[1] Japanese Standards Association 2012 *JIS G 5502 Spheroidal Graphite Iron Castings* pp 1880-

97
[2] Umetani T, Ikeda T, Sura N, Ashizuka K, Nemoto T, Takada H and Ogi K 2014 Tensile strength, fatigue strength and impact strength of solution strengthend high silicon ferritic ductile cast iron *Journal of Japan Foundry Engineering Society* **86** 36-42
[3] Ikeda T, Umetani T, Kai N, Noda N-A and Sano Y 2016 Strain rate and temperature insensitiveness of notch-bend strength for high Si ductile cast iron *ISIJ International* **56** 868-74
[4] Noda N-A, Ohtuka H, Ando M, Sano Y, Takase Y, Shinozaki T and Guan W 2013 Analysis of dynamic stress concentration and strain rate concentration for notched specimens used for high speed tensile test *Transactions of the Japan Society of Mechanical Engineers Series A* **79** 1182-90
[5] Ando H, Noda N-A, Kuroshima Y, Ishikawa Y and Takeda H 2014 Impact properties of polydimethylsiloxane copolymerized polycarbonate and application of the time-temperature superposition principle *Transactions of the JSME* **80** doi: 10.1299/transjsme. 2014smm0149
[6] Noda N-A, Ohtsuka H, Zheng H, Sano Y, Ando M, Shinozaki T and Guan W 2015 Strain rate concentration and dynamic stress concentration for double-edge-notched specimens subjected to high-speed tensile loads *Fatigue & Fracture of Engineering Materials & Structures* **38** 125-38
[7] Noda N-A, Shen Y, Takaki R, Akagi D, Ikeda T, Sano Y and Takase Y 2017 Relationship between strain rate concentration factor and stress concentration factor *Theoretical and Applied Fracture Mechanics* https://doi.org/10.1016/j.tafmec.2017.05.017
[8] Noda N-A, Akagi D, Shen Y, Takaki R, Ikeda T, Sano Y and Takase Y 2017 Strain rate concentration factor in comparison with stress concentration factor of a circumferential notch in a round bar specimen *Transactions of the JSME* **83** doi: http://doi.org/10.1299/transjsme.17-00034
[9] Ikeda T, Umetani T, Kai N, Ogi K, Akagi D, Noda N-A and Sano Y 2017 Notch strength of high silicon ductile cast iron and wide applicability to structural design *Transactions of the JSME* **83** doi: http://doi.org/10.1299/transjsme.16-00455
[10] Bennett P E and Sinclair G M 1966 Parameter representation of low-temperature yield behavior of body-centered cubic transition metals *Transactions of the ASME* **65** 518-24
[11] Fuji E, Ohkuma Y, Kawaguchi Y and Tsukamoto M 1985 Effects of temperature and strain rate on dynamic fracture toughness of steel *The Society of Naval Architects of Japan* **158** 619-29
[12] Goto K, Hirasawa H and Toyosada M 1994 A simple estimating method of constitutive equation for structural steel as a function of strain rate and temperature *The Society of Naval Architects of Japan* **176** 501-7
[13] Yamamoto H, Kobayashi T and Fujita H 1999 Strain rate-temperature dependency of impact tensile properties and ductile fracture behavior in ductile cast iron *Tetsu-to-Hagané* **85** 765-70
[14] Minami F, Hashida T, Toyoda M, Morikawa J, Ohmura T, Arimochi K and Konda N 1998 *The Society of Naval Architects of Japan* **184** 453-63
[15] British Standards Institution 2011 *EN1563Founding-Spheroidal Graphite Cast Iron* pp 23-6
[16] Larker R 2009 Solution strengthened ferritic ductile iron ISO 1083/JS/500-10 provides superior consistent properties in hydraulic rotators *China Foundry* **6** 343-51
[17] Larker R 2011 Paradigm shift in revised EN 1563 (GJS) enables improved properties and production economy in both as-cast and austempered (ADI) states *Proc. NEWCAST Forum* (Düsseldorf: Bundesverband der Deutschen Gießerei Industrie ed.) pp 29-34
[18] Löblich H and Stets W 2014 Die Einführung von mischkristallverfestigtem Gusseisen mit Kugel-graphite in die Industrie-eine Erfolgsstory *Proc. Deutscher Gießereitag 2013 und 5. NEWCAST Forum* (Fellbach: Verein Deutscher Giessereifachleute ed) pp 14-7